ISSN: 0973-3469, Vol.20, No.(1) 2023, Pg. 41-49

Material Science Research India

www.materialsciencejournal.org

Application of Calcium Hexaferrite as Microwave Absorbing Material: Review

N. M. GAHANE[1]*, Y.D. CHOUDHARI[2], P. J. CHAWARE[2] and K.G. REWATKAR[2]

[1]Department of Physics, Hislop College, Nagpur.
[2]Department of Physics, Dr. Ambedkar college, DeekshaBhoomi, Nagpur, India.

Abstract

Many studies have been conducted on Spinel, Garnet, and Hexa-ferrites in single and multi-doped concentrations. This article is an attempt to review the researcher's work on Ca, Ba, and Sr hexaferrite by substituting a variety of various ions such as Al, La, Sn, Zr, Co, Cr, and Ir. This review paper investigates M-type (Ca, Sr, Ba) Hexa-ferrites with a space group of P63/mmc that were synthesized using various techniques and characterized by XRD for crystallographic information, SEM and TEM for surface morphology, VSM for magnetic behaviour, and Vector Network Analyzer (VNA) for microwave absorption properties. Changes in a material's chemical composition affect features such as coercivity, saturation magnetization, and Curie temperature, as well as managing these properties and utilizing these compounds in the field of microwave absorption properties and magnetic field industry.

Article History
Received: 24 January 2023
Accepted: 24 February 2023

Keywords
coercivity, Hexaferrite; magnetization; Saturation; SEM; VNA; XRD; etc.

Introduction

Numerous studies have been conducted since the invention of radar to create radar-absorbing materials. This material is beneficial for antenna pattern shaping, radar cross reduction, and EMI reduction. The radar absorbing materials work by absorbing radar electromagnetic radiation.[1] The magnetic and dielectric properties of the materials influence the absorption of the E-M wave. The absorbing material must have the lowest reflectance throughout the largest bandwidth, the weight and size of the absorbing material are also critical for radar. Radar absorption materials are divided into two types, conductive materials and magnetic materials.[2] Hexa-ferrites and carbonyl iron are used in magnetic radar absorbers. Hexaferrite is a type of hard ferrite that is a permanent magnet that retains its magnetism after being magnetized and has a high coercivity and remanence after magnetization.[3] Certain ferrites are further split into the following groups: M, W, Y, Z, and X compounds. Each of them possesses a unique crystalline phase via which absorption materials have been absorbed in the MHz and GHz band ranges.[4] The performance

CONTACT N. M. Gahane pritichaware@gmail.com Department of Physics, Hislop College, Nagpur.

© 2023 The Author(s). Published by Enviro Research Publishers.
This is an Open Access article licensed under a Creative Commons license: Attribution 4.0 International (CC-BY).
Doi: http://dx.doi.org/10.13005/msri/200105

of a material is determined by its structure and physical qualities. Changing the chemical makeup of an absorber can result in significant changes in chemical and physical properties across a wide range of frequency bands.[5] There have been no publications published on M-type barium ferrites or strontium ferrites, although there have been a few studies on the microwave absorption magnetic characteristics of calcium hexaferrite. As a result, we took up the review paper for calcium hexaferrite.[6]

Table 1: Classification of hexaferrite

Hexaferrite type	Combination	Molecular formula	Structural Staking
M	M	$CaFe_{12}O_{19}$	RSR*S*
Y	Y	$CaSrFe_{12}O_{19}$	TSTSTS
W	M+S	$CaCo_2Fe_{16}O_{27}$	RSSR R*S*S*
Z	M+Y	$Ca_3\ Co_2Fe_{24}O_{41}$	RSTSR*S*T*S*
X	2M+S	$Ba_2\ Co_2Fe_{28}O_{46}$	RSR*S*S*

Table 2: Crystallographic site of hexaferrite

Sub lattice	Coordination	Block	No of ions	Spin orientations
2a	Octahedral	S	one	↑
2b	Pseudo-tetrahedral	R	one	↑
4fIV	tetrahedral	S	two	↓
4fIV	Octahedral	R	two	↓
12K	Octahedral	R-S	six	↑

Experimental Technique

The sol-gel technique, coprecipitation method, hydrothermal method, and solid-state method are easy chemical ways for economically producing hexagonal ferrites. These techniques are effective for regulating the grain size and morphology of ferrite particles.[7] When creating a ferrite powder, we pay close attention to the following factors: Heat treatment, chemicals used in beginning powders, powder stoichiometry Using these crucial components, the Ca hexaferrite material was substituted with Mg-Ti, and several hexaferrite samples were generated using the citrate sol-gel method.[8] Between the frequencies of 12 and 20 GHz, the microwave absorption characteristics of calcium hexaferrite replaced by Mg-Ti were investigated. Similarly, the Ca substituted Sr hexaferrite was produced using a standard solid-state reaction approach [9], before being applied in magnetic media and absorbing microwaves. For the field of high-density recording media, the Sn-Zr substituted Ca hexaferrite was synthesized using the sol-gel auto combustion process with urea as a fuel.[10] The Co-Sn and Sn-Zr substituted Ca hexaferrite with the chemical formulas Ca(Co-Sn) $xFe_{12-2x}O19$ and Ca(Co-Zr) $xFe_{12-x}O19$ for x= 0 to 5 were synthesized by sol-gel technique.[11] The M Type Ba hexaferrite substituted by Ca generated by microemulsion and a stearic acid sol-gel method is useful in the storage media industry. Previously, Ir-Co substituted Ca hexaferrite with the chemical formula $CaFe_{12-2x}IrxCoxO_{19}$, which was manufactured using the chemical-coprecipitation process.[12] The microwave absorption capabilities of calcium and strontium hexaferrite substituted with Co and Ti by boll milling technique and solid-state reaction were investigated at frequencies ranging from 8.4 GHz to 12.4 GHz. A ceramic approach was used to create the Cu-Ti and Al-Co substituted M Type Ca hexaferrite for x=0 to 5 and x=2 to 5.[13,14]

Results and Discussions

XRD Report

The sol-gel method, solid-state reaction, ceramic process, and coprecipitation method were all used to successfully synthesis the M-type Calcium

hexaferrite nanoparticle. X-ray diffraction studies reveal the creation of a hexagonal structure with a space group of P63/mmc and planes (107), (114), (203), and (204 (108).[15] The lattice parameters were discovered to be in the range of a = 5-6 and c = 22-24. The Debye-Scherer formula was used to determine the particle's averaged crystallite size.[16] The TEM pictures revealed that the produced ferrites nanoparticles were spherical with a size distribution between 20 and 60 nm, which corresponded to the particle size determined by XRD. Due to unit cell elongation, bigger La, Mg–Ti, Sn–Zr, Cu-Ti, Co-Ti, Co-Sn, and Co-Al ions are replaced by smaller Fe ions.[17,18]

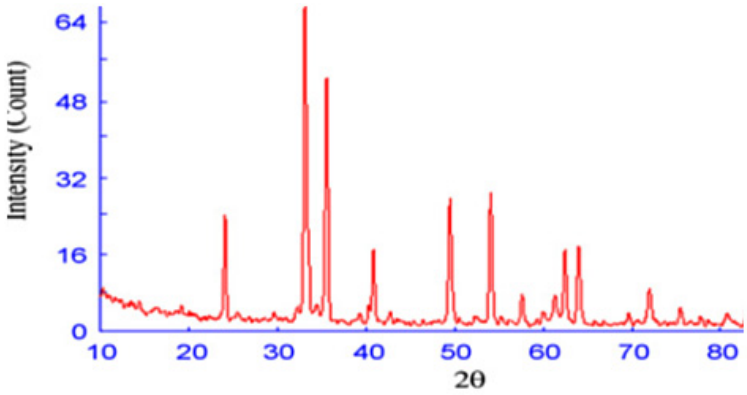

Fig. 1: XRD image of M-type hexaferrite

Table 3: Lattice parameter, particle size of Hexaferrite

Hexaferrite material	a (Å)	c (Å)	crystalline size (nm)	Volume Å^3
Ca(Co–Sn)0.2Fe11.6O19	5.843	21.516	56.17	636.137
$SrFe_{12}O_{19}$	5.641	22.322	54.17	654.345
$CaLa_{0.7}Fe_{11.3}O_{19}$	5.621	22.361	24	635.24

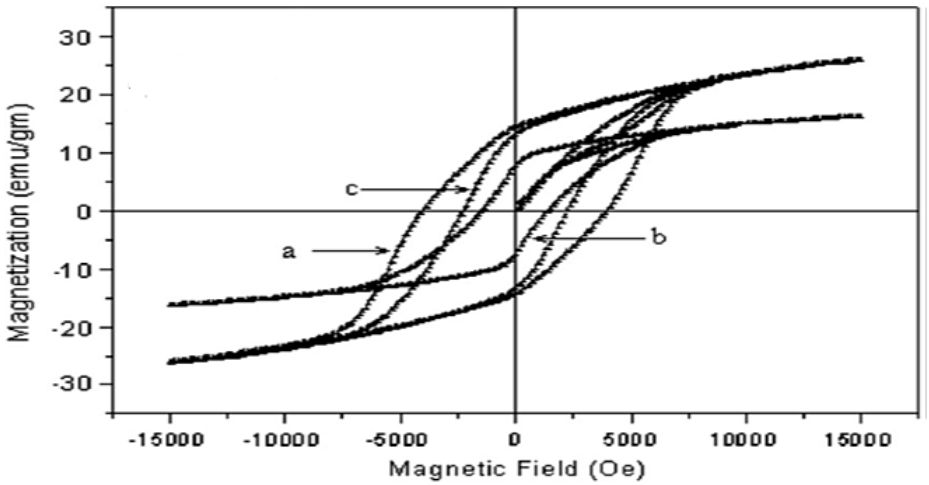

Fig. 2: VSM Graph of M-type hexaferrite

VSM Report

The magnetic properties of the material, such as saturation magnetization, coercivity (Hc), and Retentivity (Mr), proved its hard ferrite nature. When a material is used for storage, its coercivity is important.[19] As the concentration of replacing ions in the material increases/decreases, if the coercivity is low, it becomes a soft magnet, if the coercivity is high, it becomes a hard magnet. The Fe^{3+} ions in the M-type hexaferrite composition are dispersed in five separate crystallographic locations: three up-spin sites (2a, 12k, and 2b) and two down-spin sites (4f1 and 4f2) along the c axis.[20] The saturation magnetization and coercivity were observed to decrease with increasing Mg-Ti concentrations, while increased with increasing Al concentrations using hysteresis loops.[21] The activation energy and dc electrical resistivity of ferrite samples increased with increasing Al concentration at room temperature. In the presence of surfactants, Ba-Ca hexaferrite exhibited low coercivity.[22]

Table 4: Ms, Mr of M-type Hexaferrite.

Sample	Saturation magnetization (Ms)	Remnant magnetization (Mr)	Neel temperature (k)	Tc (k)
$BaFe_{12}O_{19}$	4760–4775	3640–3700	447	650-750
$CaFe_{12}O_{19}$	2200-3250	1700–2600	450	450-650
$SrFe_{12}O_{19}$	3450–3570	3400–3500	456	700-800

The appearance of non-magnetic anions in the tetrahedral and octahedral positions was frequently responsible for the low Curie temperature. Sites 2a and 2b, 12k, and 4f have been occupied by non-magnetic ions such as magnesium, titanium, copper, and aluminum.[23]

SEM

SEM images of fragmented surfaces of La substituted sintered Ca hexaferrite are shown in the figure. The micrograph demonstrates that the particle size is reduced as a result of La replacement. Hexaferrite of calcium was used in place of the original substance. The index of crystallinity was derived from the following relationship.[24] A micrograph gives us the average particle size of D, while a Scherer equation tells us the average crystalline size of r. The pinning effect and particle growth inhibition may be caused by a little amount of unsubstituted La2O3 in the sample.[25]

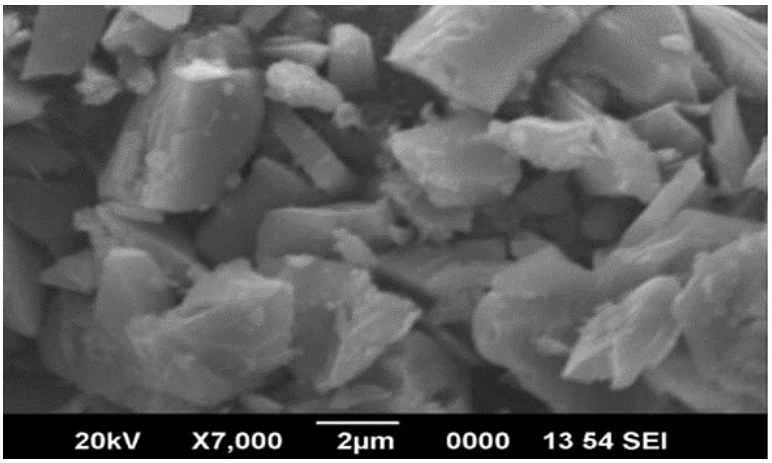

Fig. 3: SEM Micrograph of $CaLaXFe_{12-x}O_{19}$

Microwave Absorbing Property

The reflection loss (RL) of hexaferrite materials was used to investigate their microwave absorption capabilities; as a result, the preceding formula can be used to calculate reflection loss

$$RL(dB)=20 \log[(Zin-1)/(Zin+ 1)] \quad ...(1)$$

$$Zin=\sqrt{(u/\varepsilon)} \tan h(j\, 2\pi fd/c \sqrt{u\varepsilon}) \quad ...(2)$$

Where f is the microwave frequency, d is the absorber layer thickness, and c is the velocity of an electromagnetic wave in a vacuum. and u are the complex relative permittivity and permeability, respectively, while Zin is the absorber's input impedance.[26] The microwave absorption property of material was tested between 3 and 12 GHz, which requires a low matching thickness, low reflection loss, and a wide absorption bandwidth. When it comes to storing electric and magnetic energy, the real portions of complex permittivity (ε′) and permeability (u′) are used, while the shadowy portions of complex permittivity (ε″) and permeability (u″) have been used to express the dissipation of magnetic and electrical energy.[27] It is useful for microwave absorption if the absorbers have large imaginary portions of both complex permittivity and permeability, as reflection loss is impacted by impedance. As a result, to accomplish impedance matching, the real components (ε′ and μ′) must be as identical as possible.[28] The imaginary parts of Ba hexaferrite are very close to one and zero, while the real parts are close to 2–27. For frequencies between 2 and 18 gigahertz, has a very minor change, this indicates that it has a very low dielectric loss.[29]

Table 5: Reflection loss, layer size of Hexaferrite.

Material	Layer Size (Mm)	Frequency Range(Ghz)	Reflection Loss (Db)	Reference
Ba hexaferrite ($BaFe_{12}O_{19}$)	2mm-3mm	8-14.8	-30 to -17	[17] [31] [35]
Sr hexaferrite ($SrFe_{12}O_{19}$)	1mm-2mm	8-12	-16 to -8	[20] [26]
Ca hexaferrite ($CaFe_{12}O_{19}$)	2mm- 3 mm	8- 20	-39 to -.9	[1][9]

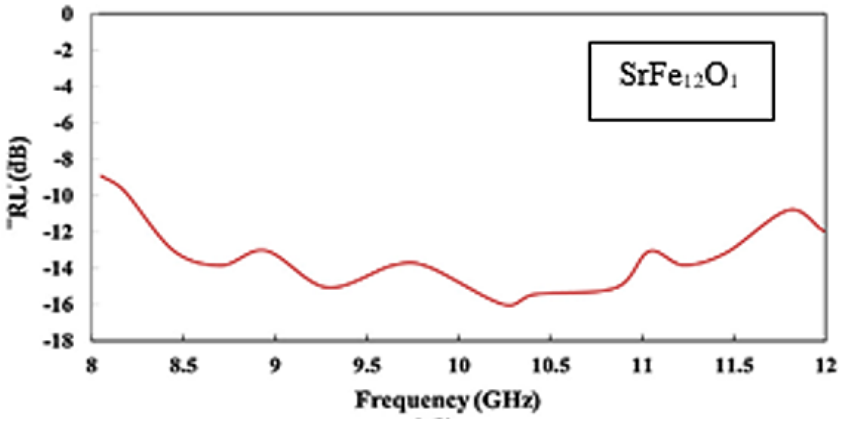

Fig. 4: Reflection loss of M-type hexaferrite

Whenever the RL is below -10 decibels, only 10% of the electromagnetic radiation has mirrored, whereas 90% of the electromagnetic energy consumed. The effective absorption bandwidth is established for a certain frequency range when RL is less than -10 dB.[30] When the thickness of the absorber is changed, the greatest absorption peaks shift to a lower frequency.[31] The electrical test demonstrates the bandgap calculation for the material, which effectively provides a significant choice for microwave absorption. The detailed energy calculation is performed as follows.

Eg=(2k*2.3026*logρ)/(1/T) ...(3)

When it comes to matching width, there is a frequency at which the two pieces of information peer. When replacing magnetic Fe^3 with non-magnetic ions, the matching frequency drops almost exponentially, which would conflict with a drop in the anisotropy field as the substitution level progress.[32] The reflection coefficient of Ca hexaferrite decreased with increasing applied field frequency, as seen in figure 5. The Sr-Ca hexaferrite possesses low conductivity, low dielectric constant (ε′′), and dielectric loss tangent (tan δ).

Table 6: Electrical parametric value of sample

Sample	Band Gap Eg (ev)	Resistivity (at RT 34^{0}C)	Transition Tem. K)	Volume (A^3)
$Ca0.7Sr_{0.3}Fe_{12}O_{19}$	0.380	2.212*107	409	644.242
$SrFe_{12}O_{19}$	0.23	2.322*107	413	654.345
$CaLa_{0.7}Fe_{11.3}O_{19}$	0.24	2.33*107	408	635.24

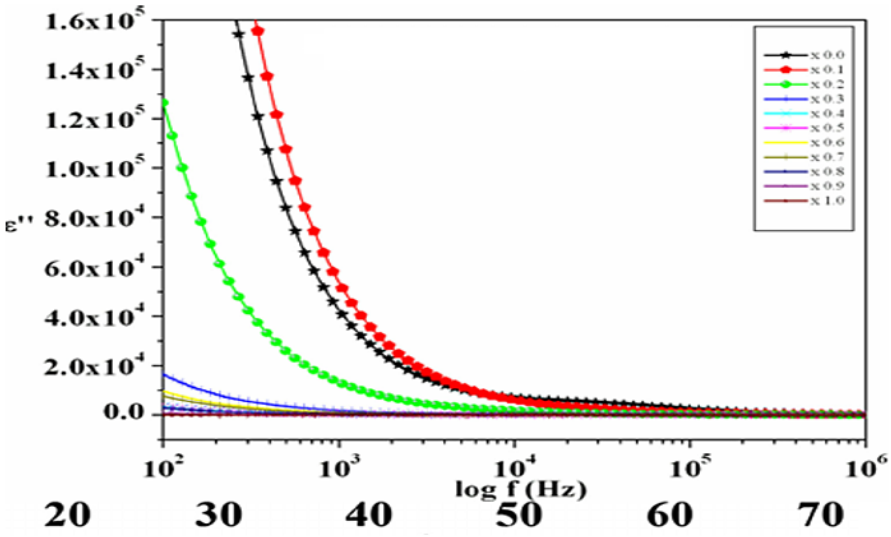

Fig. 5 : Variation of dielectric with frequency

Conclusion

Ca hexaferrite has a very fascinating subject of research for scientists because of its data storage and microwave uses. The substitution of various ions in Ca hexaferrite resulted in promising modifications in the electrical, magnetic, and physical characteristics, indicating that the researcher can manufacture new M-type hexaferrite with improved attributes through impurity substitution. The current review concludes that calcium hexaferrite is suitable for microwave absorption and a very good replacement for barium and strontium hexaferrite, as it exhibits extremely similar features Ba and Sr. There is numerous research that must be conducted utilizing various methods of preparation of Ca hexaferrite, with varied ferrite compositions, to determine the effect of preparation procedures on the properties of ferrite. The energy band gap of La-substituted powders and sintered pellets is evaluated using the four-probe method, which demonstrates that the sample's resistivity and energy bandgap decrease as the conversion rate for lanthanum rises. The Scherer formula is used to determine particle size. Lanthanum substitution increases with particle size. The temperature-recorded M-H curves revealed that large values of Ms, Mr, and Hc were

obtained for all $Ca_{1-x}SrxFe_{12}O_{19}$ nanoribbons and that they increased with ribbon-width broadening. Specifically, the best Ms and Hc were around 67.9 emu/g and 7.31 kOe.

Acknowledgment

The author would thankful for the Department of Nanoscience and Nanotechnology Dr. Ambedkar College, Nagpur for providing synthesis and electrical characterizations and VMV college for proving the setup for random measurement of Energy band gap using electronic setup.

Funding

The author(s) received no financial support for the research, authorship, and/or publication of this article.

Conflict of Interest

The author wouldn't have any conflict of interest with other authors. This is finding with the sample; the result may be changed with combinational concentration

References

1. Y. Taryana, W. A. Adi, D. Mahmudin, Y. Wahyu, and A. Manaf, "Structural, magnetic and microwave absorption characteristics of ba1-xlaxfe12o19 (X = 0; 0.1; 0.2;0.3;0.5;0.7)," *Key Engineering Materials,* vol. 855 KEM, pp. 261–267, 2020, doi: 10.4028/www.scientific.net/KEM.855.261.
2. M. A. Almessiere *et al.,* "Alterations in the magnetic and electrodynamic properties of hard-soft Sr0.5Ba0.5Eu0.01Fe12O19/NixCuyZnwFe2O4 nanocomposites," *Journal of Materials Research and Technology,* vol. 15, pp. 1416–1429, 2021, doi: 10.1016/j.jmrt.2021.08.137.
3. A. Kumar, P. Sharma, and D. Varshney, "Structural and dielectric properties of Nd/Ca co-doped bi-ferrite multiferroics," *AIP Conference Proceedings,* vol. 1591, pp. 40–41, 2014, doi: 10.1063/1.4872481.
4. Y. D. Choudhari and K. G. Rewatkar, "Influence of Bi3+ ions substitution on structural, magnetic, and electrical properties of lead hexaferrite," *Journal of Magnetism and Magnetic Materials,* vol. 551, Jun. 2022, doi: 10.1016/j.jmmm.2022.169162.
5. K. G. Rewatkar, N. M. Patil, S. Jaykumar, D. S. Bhowmick, M. N. Giriya, and C. L. Khobragade, "Synthesis and the magnetic characterization of iridium-cobalt substituted calcium hexaferrites," *Journal of Magnetism and Magnetic Materials,* vol. 316, no. 1, pp. 19–22, 2007, doi: 10.1016/j.jmmm.2007.03.192.
6. A. K. Nandanwar, N. N. Sarkar, D. S. Choudhary, D. K. Sahu, and K. G. Rewatkar, "ScienceDirect Effect of Ni +2 Substitution on Structural and Electrical Behaviour of Nano-Size Cadmium Ferrites," 2017.
7. Y. D. Choudhari and K. G. Rewatkar, "Materials Today: Proceedings," no. xxxx, pp. 1–8.
8. A. Sharbati and G. R. Amiri, "Magnetic, microwave absorption and structural properties of Mg–Ti added Ca–M hexaferrite nanoparticles," *Journal of Materials Science: Materials in Electronics,* vol. 29, no. 2, pp. 1118–1122, 2018, doi: 10.1007/s10854-017-8013-0.
9. A. Hooda, S. Sanghi, A. Agarwal, and R. Dahiya, "Crystal structure refinement, dielectric and magnetic properties of Ca/Pb substituted SrFe12O19 hexaferrites," *Journal of Magnetism and Magnetic Materials,* vol. 387, pp. 46–52, 2015, doi: 10.1016/j.jmmm.2015.03.078.
10. H. A. N. Zhidong, D. Limin, Z. Dawei, W. U. Ze, and Z. Xianyou, "Synthesis of BaFe12019 / MFe20 ,(M = Co , Mn) by sol-gel method," vol. 2, pp. 462–465, 2006.
11. G. Ferk *et al.,* "Monolithic magneto-optical nanocomposites of barium hexaferrite platelets in PMMA," *Scientific Reports,* vol. 5, pp. 1–8, 2015, doi: 10.1038/srep11395.
12. G. B. Teh, N. Saravanan, and D. A. Jefferson, "A study of magnetoplumbite-type (M-type) cobalt-titanium-substituted barium ferrite, BaCoxTixFe12-2xO19 (x = 1-6)," *Materials*

Chemistry and Physics, vol. 105, no. 2–3, pp. 253–259, Oct. 2007, doi: 10.1016/j.matchemphys.2007.04.054.

13. S. Pignard, H. Vincent, E. Flavin, and F. Boust, "Magnetic and electromagnetic properties of RuZn and RuCo substituted BaFe12O19," *Journal of Magnetism and Magnetic Materials,* vol. 260, no. 3, pp. 437–446, Apr. 2003, doi: 10.1016/S0304-8853(02)01387-2.
14. P. D. Popa, E. Rezlescu, C. Doroftei, and N. Rezlescu, "Influence of calcium on properties of strontium and barium ferrites for magnetic media prepared by combustion," *Journal of Optoelectronics and Advanced Materials,* vol. 7, no. 3, pp. 1553–1556, 2005.
15. W. Alexiewicz and K. Grygiel, "Cole-cole plots for linear and nonlinear dielectric relaxation in solutions of rigid, highly dipolar, symmetric-top molecules in spherical solvents," *Acta Physica Polonica A,* vol. 114, no. 4, pp. 687–698, 2008, doi: 10.12693/APhysPolA.114.687.
16. S. Mukherjee, K. Sarkar, and S. Mukherjee, "Effect of nickel and cobalt doping on nano bismuth ferrite prepared by the chemical route," *InterCeram: International Ceramic Review,* vol. 64, no. 1, pp. 38–43, 2015, doi: 10.1007/bf03401099.
17. J. Sláma *et al.,* "Magnetic properties of Me-Zr substituted Ba-hexaferrite," *Journal of Magnetism and Magnetic Materials,* vol. 272–276, no. I, pp. 385–387, 2004, doi: 10.1016/j.jmmm.2003.11.156.
18. T. M. Clark and B. J. Evans, "Mössbauer investigation of M-type hexaferrites above their Curie temperatures," *Journal of Magnetism and Magnetic Materials,* vol. 177–181, no. PART 1, pp. 237–238, 1998, doi: 10.1016/S0304-8853(97)00319-3.
19. A. S. Kakde, B. A. Shingade, N. S. Meshram, and K. G. Rewatkar, "STRUCTURAL AND MAGNETIC PROPERTIES OF SN-ZR SUBSTITUTED CALCIUM NANO-HEXAFERRITE .," vol. 1, no. 2, pp. 60–63, 2014.
20. C. S. Prakash, N. N. Sarkar, A. S. Kakde, K. G. Rewatkar, V. M. Nanoti, and P. Shesu, "Super-paramagnetic Iron Oxide Nanoparticles for Hyperthermia Applications Super-paramagnetic Iron Oxide Nanoparticles for Biomedical (Hyperthermia) Applications."
21. J. Massoudi *et al.,* "Magnetic and spectroscopic properties of Ni-Zn-Al ferrite spinel: From the nanoscale to microscale," RSC Advances, vol. 10, no. 57, pp. 34556–34580, 2020, doi: 10.1039/d0ra05522k.
22. C. Mamatha, M. Krishnaiah, and C. S. Prakash, "Structural, Electrical and Magnetic properties of Aluminum Substituted Nanocalcium Hexaferrites," vol. 6, no. 3, pp. 2165–2167, 2014.
23. F. Ansari and M. Salavati-niasari, "Simple sol-gel auto-combustion synthesis and characterization of Lead Hexaferrite by utilizing cherry juice as a novel fuel and green capping agent," pp. 1–24.
24. M. Siva Ram Prasad, K. V. Ramesh, B. R. Babu, and K. Trinath, "DC electrical resistivity and dielectric properties of Ni–Zn nanoferrite synthesized via autocombustion route," *Indian Journal of Physics,* vol. 90, no. 4, pp. 417–428, 2016, doi: 10.1007/s12648-015-0773-x.
25. S. Sagadevan, Z. Z. Chowdhury, and R. F. Rafique, "Preparation and characterization of nickel ferrite nanoparticles via co-precipitation method," *Materials Research,* vol. 21, no. 2, pp. 21–25, 2018, doi: 10.1590/1980-5373-mr-2016-0533.
26. H. K. Choudhary, S. P. Pawar, S. Bose, and B. Sahoo, "EMI shielding performance of lead hexaferrite/polyaniline composite in 8-18 GHz frequency range," *AIP Conference Proceedings,* vol. 1953, 2018, doi: 10.1063/1.5033126.
27. A. Houbi, Z. A. Aldashevich, Y. Atassi, Z. Bagasharova Telmanovna, M. Saule, and K. Kubanych, "Microwave absorbing properties of ferrites and their composites: A review," *Journal of Magnetism and Magnetic Materials,* vol. 529, no. September 2020, p. 167839, 2021, doi: 10.1016/j.jmmm.2021.167839.
28. J. Liu and X. Xue, "Morphology and magnetic properties of SrFe12O19 synthesized with oxidized scale," *Materials Letters,* vol. 164, pp. 579–582, 2016, doi: 10.1016/j.matlet.2015.11.026.
29. A. Katoch, B. K. Borthakur, A. Singh, and T. Singh, "Dielectric Behavior of M-Type

Hexaferrites Sr 1-x Dy x Fe 12 O 19 Doped with Rare Earth Ions," vol. 5, no. 1, pp. 53–57, 2013.

30. M. Tuhkala *et al.,* "The effect of BaTiO3 particle shape on complex permittivity of 0.98MgTiO3-0.02BaTiO3 composite powders at GHz frequencies," *Materials Research Bulletin,* vol. 76, pp. 300–304, 2016, doi: 10.1016/j.materresbull.2015.12.043.
31. H. Dubey, C. Verma, U. Rai, A. Kumar, and P. Lahiri, "Synthesis, characterization and properties of nickel based zinc ferrite nanoparticles," *Indian Journal of Chemistry -Section A (IJC-A),* vol. 58, no. 04, pp. 454–458, 2019.
32. N. Humera, S. Riaz, and S. Naseem, "Effect of temperature on electrical properties of barium titanate nanoceramics," vol. 5, no. c, pp. 153–161.